An Assessment of the impact of the 1997-98 El Niño on the Asian-Australian monsoon

K.-M. Lau[1] and H.-T. Wu[2]

Laboratory for Atmospheres,

NASA/Goddard Space Flight Center

Greenbelt, 20771, Maryland, USA

(Submitted to *Geophysical Research Letters*)

January 1999

[1] *Corresponding author*: Dr. W. K.-M. Lau, Laboratory for Atmospheres, NASA/GSFC, code 913, Greenbelt, MD 20771. Email: lau@climate.gsfc.nasa.gov

[2] S M & A Corporation, 901 Follin Lane, Suite 400, Vienna, VA 22180

1

Abstract

Using state-of-the-art satellite-gauge monthly rainfall estimate and optimally interpolated sea surface temperature (SST) data, we have assessed the 1997-98 AA-monsoon anomalies in terms of three basic causal factors: basin-scale SST, regional coupling, and internal variability. Singular Value Decomposition analyses of rainfall and SST are carried out globally over the entire tropics and regionally over the AA-monsoon domain. Contributions to monsoon rainfall predictability by various factors are evaluated from cumulative anomaly correlation with dominant regional SVD modes. Results reveal a dominant, large-scale monsoon-El Niño coupled mode with well-defined centers of action in the near-equatorial monsoon regions during the boreal summer and winter respectively. The observed 1997-98 AA-monsoon anomalies are found to be very complex with approximately 34% of the anomalies of the Asian (boreal) summer monsoon and 74% of the Australia (austral) monsoon attributable to basin-scale SST influence associated with El Niño. Regional coupled processes contribute an additional 19% and 10%, leaving about 47% and 16% due to internal dynamics for the boreal and austral monsoon respectively. For the boreal summer monsoon, it is noted that the highest monsoon predictability is not necessary associated with major El Niño events (e.g. 1997, 1982) but rather in non-El Niño years (e.g. 1980, 1988) when contributions from the regional coupled modes far exceed those from the basin-scale SST. The results suggest that in order to improve monsoon seasonal-to-interannual predictability, there is a need to exploit not only monsoon-El Niño relationship, but also intrinsic monsoon regional coupled processes.

1. Introduction

Arguably the strongest and certainly the most hyped climate anomaly of this century, the 1997-98 El Niño was the cause of a record number of major weather related disasters around the world. El Niño related impacts on the Asian-Australian (AA) region can be particularly devastating because the region sustains over 60% of the world population whose livelihood is at the mercy of the vagaries of the monsoon climate. It is well known that while El Niño may impact the AA-monsoon, severe droughts and floods in the region can be due to other factors (Rasmussen and Carpenter 1983, Webster et al. 1998). Recently, Lau et al. (1998), hereafter referred to as LKY, proposed a characterization of AA-monsoon interannual anomalies according to three fundamental causal factors: (a) global processes such as El Niño and climate change, (b) regional ocean-land-atmosphere coupling, and (c) internal dynamics. They suggested that predictability of the AA-monsoon could be enhanced by better understanding and exploiting physical processes in (a) and (b) and their mutual interactions. In this paper, we describe a methodology and present results aiming at a quantitative estimate of the relative roles of these factors in contributing to the observed 1997-98 AA-monsoon anomalies. Detailed discussion of the regional anomalies and their physical mechanisms will be presented in a separate paper.

2. Data and methodology

For sea surface temperature (SST) we used the National Centers for Environmental Prediction (NCEP) optimally interpolated SST at 2° x 2° resolution, for the period January 1979-February 1998 (Reynolds and Smith 1994). For precipitation, we used the Global Precipitation Climatology Project (GPCP) Version 1a, gauge-satellite merged products (Huffman et al. 1997), and the Climate Prediction Center Merged Analysis of Precipitation (CMAP) (Xie and Arkin 1996). The CMAP and the GPCP rainfall amounts and anomaly patterns are very similar. The

3

GPCP data currently available covers the period from January 1987 to February 1998 and the CMAP data from January 1979 to January 1998. Identical analyses have been carried out for both rainfall products. For brevity, the intercomparison between the rainfall data sets will not be presented here. Suffice it to say that the two rainfall products yield very little differences in the present results.

3. 1997-98 tropical rainfall and SST anomalies

During JJA 1997, the SST anomaly pattern (Fig. 1a) was quite typical of an El Niño. A tongue of abnormally warm water was found over the eastern equatorial region, reaching a maximum (> 4°C) off the coast of Peru. The cold anomaly was much weaker but more widespread, extending from the equatorial western Pacific to the subtropics of both hemispheres. Except for the extreme equatorial eastern portion, and some portion of the central southern region, SST over Indian Ocean was generally above normal. In the rainfall field (Fig. 1b), the Intertropical Convergence Zone (ITCZ) over the eastern Pacific was shifted southward over the equator. Over the Indo-Pacific sector, the precipitation pattern was very complex. While rainfall was suppressed in the near equatorial regions from Papua New Guinea to the eastern and central Indian Ocean, and central East Asia, it was enhanced over the west coast of India, the Bay of Bengal, and the coasts of Indochina and south China. These features were generally consistent with the widespread floods and droughts reported in these regions during 1997 boreal summer (WMO Climate Bulletin 1997). Note that because of the complex nature of the rainfall pattern, a geographic average over a small region such as the Indian subcontinent clearly was not representative of the anomalies of the entire AA-monsoon region.

4

As the El Niño evolved, the warm water region over the eastern equatorial Pacific intensified and expanded. Meanwhile, a secondary cold tongue appeared over the equatorial Indian Ocean off the coast of Sumatra in July and peaked in October 1997 (not shown). Associated with this cold tongue development was significant warming of the central and western Indian Ocean, which intensified and spread over the entire basin from October through February, reaching a magnitude of over $1.5^\circ - 2^\circ C$ in the equatorial western Indian Ocean and southeastern Indian Ocean respectively (Fig. 1c). As noted by other authors, the extent and magnitude of the warming of the Indian Ocean during 1997 was unprecedented (Webster et al. 1998). In the DJF rainfall anomaly field (Fig. 1d), extensive regions with deficit rainfall were found over the western Pacific, the South Pacific Convergence Zone (SPCZ), the eastern Indian Ocean, and northern Brazil. These rainfall-deficit regions engulfed a large area of enhanced rainfall over the equatorial central and eastern Pacific. Additionally, there was substantial increase in rainfall over eastern Africa and the western Indian Ocean. In a smaller area confined to northern Australia and the Timor Sea enhanced rainfall was also observed.

4. Global vs. regional impacts

Given the complex nature of the 1997-98 AA-monsoon rainfall anomalies, a natural question to ask is how much of the observed anomalies are due to El Niño and how much arise from other causes. To attribute causes for the observed 1997-98 AA-monsoon anomalies, we have computed dominant patterns of covariability between monthly rainfall and SST for the 19-year period from 1979 to 1998, using Singular Value Decomposition (SVD) for the boreal summer (May through September, MJJAS) and for the austral summer (October through February, ONDJF). To isolate

the regional and global influence, the SVD's are computed separately over the global extended tropics (40°S – 40°N) and the AA-monsoon domain (40°S –40°N, 30° E – 150°E).

a. The boreal monsoon

Table 1 shows the percentages of covariance explained by the global and the regional SVDs within their respective domains for MJJAS. As evident in the large proportion of covariance (58.4% of the squared covariance) explained by the first global SVD, there is a well-defined dominant global coupled SST-rainfall mode. Except for the detailed features within the AA-monsoon region, the SST and rainfall patterns of the first global SVD (Figs. 2a and b) are broadly similar to those shown in Fig. 1 and can be clearly identified with those associated with El Niño. In the rainfall pattern (Fig. 2b), the El Nino influence is consistent with a broad region of descending motion (rainfall deficit) associated with an anomalous Walker circulation, with centers of action over Indonesia, the Philippines/ western subtropical Pacific, and the eastern equatorial Indian Ocean. Positive rainfall centers are also found over the Bay of Bengal and southern East Asia. Note again that the Indian subcontinent is *not* a center of action of El Niño.

For the regional SVDs, the covariances are spread out among the first three coupled modes (29.3%, 15.8% and 12.7% respectively), which are significantly separated from the higher order modes. The SST and rainfall patterns of the first regional SVD (not shown) are nearly identical to the first global SVDs in the common domain. In contrast, the second and third regional SVDs do not have counterparts in the global SVDs. The rainfall patterns of these two SVDs (not shown) are similar respectively to those associated with the monsoon subsystems of South Asia and East-South Asia as identified by LKY. Based on the above discussion, the first regional SVD can be construed as the "canonical" monsoon-El Nino mode. Without loss of generality, we shall

refer to this as the basin-scale SST mode. The second and third regional SVDs can be considered as regional coupled SST-rainfall modes. These modes stem from ocean-atmosphere-land coupling within the AA-monsoon domain and are distinct from the basin-scale SST mode.

Since there is no *a priori* criterion to determine the number of regional SVDs that are required to include all the physically meaningful covariance between monsoon rainfall and SST, we make the assumption that all the physical covariances are contained in the first five regional SVD's. Under this assumption, all higher order (>5) modes are regarded as generated by internal dynamics or noise within the AA-monsoon system. In other words, the potential predictability (assuming perfect prediction of the coupled modes) of the AA-monsoon system resides within the first five SVDs. The results presented here are insensitive to the choice of the SVD cutoff, provided the first three modes are included in potentially predictable category.

We use anomaly correlation to estimate the contribution of the various regional modes to the variability of the total monsoon system in the following way. First, we compute the anomaly (spatial) correlation between the observed rainfall and SVD projections. The cumulative contribution up to the ith SVD to the rainfall anomaly for the jth year is given by:

$$A_{i,j} = < O_j, \sum_1^i SVD(i) * PC(i)_j >,$$

$$(1)$$

where $< >$ is the anomaly correlation over the AA-monsoon domain; PC denotes the principal component and O_j the observed rainfall anomaly. The contribution of the ith SVD to the rainfall anomaly is then given by the difference formula:

$$C_{1,j} = A_{1,j} \qquad (2)$$

$$C_{i,j} = A_{i,j} - A_{i-1,j}, \quad i = 2, \ldots 5 \qquad (3)$$

7

Figure 3 shows the contribution to the cumulative anomaly correlation by the first five SVDs for different years. The cumulative anomaly correlation contributed by the first five SVDs varies between 0.3 to 0.6. Using the cumulative anomaly correlation as a limit of potential monsoon rainfall predictability based on SST, the internal dynamics which constitutes the unpredictable portion can be as high as 0.4 to 0.7. Note that the basin-scale SST contribution (blue bar) varies from year-to-year between 0.1 to 0.4, with 1997 having a relatively large ($\approx$0.35) but not the largest contribution during the past 19 years, which occurs during 1984 and 1989. Interestingly, the regional coupled modes collectively, (largely from the 2^{nd} and 3^{rd} SVD), contribute on the average about the same amount as the basin-scale SST. As expected, contributions from the 4^{th} and 5^{th} SVDs only marginally increase the anomaly correlation. It is clear that over the entire domain, the basin-scale SST exerts strong influence on the 1997 summer monsoon anomaly, with somewhat lesser but non-negligible contributions from the regional coupled modes (2^{nd} through 5^{th} SVD). The relative contribution of the basin-scale and the regional scale modes are very different in 1997 and 1982, even though both are strong El Niño years. The basin-scale SST has a large impact on the well-known weak South Asia summer monsoon of 1987. Yet the strong South Asia monsoon in 1988 appears to be underpinned by strong regional coupling (mainly through the 2^{nd} SVD), with minimal impact from basin scale SST. Worth noting is that during 1980, the overall predictability ($\approx$ 0.58) is higher than both the El Niño years of 1982 and 1997, being enhanced by the regional modes, especially the 3rd regional SVD, with relatively little contribution from the basin scale SST.

8

b. The austral monsoon

As evident in Table 2, the dominance of the first global SVD in the SST-rainfall covariability for the austral summer (ONDJF) is even more remarkable with 74.6% squared covariance explained. The SST and rainfall patterns of the first global SVD (Figs. 2c and d) are broadly similar to the observed (Figs. 1c and d). Compared to the SVD SST pattern (Fig. 2c), the 1997-98 observed SST (Fig. 1c) appears to have more extensive warm anomalies and less well developed cold anomalies over the entire tropics, especially in the Indian Ocean and the subtropical western Pacific and Atlantic. The El Nino signal in rainfall is very well defined in the SVD pattern (Fig. 2d) with a east-west equatorial dipole signaling a shift of the major austral monsoon convective zone from the western to the central Pacific. Missing in the global SVD rainfall are regional features such as the large positive anomalies over the western Indian Ocean and East Africa, enhanced rainfall over northern Australia /Timor Sea, which were very pronounced in the 1997-98 DJF observation (Fig. 1d).

Again, for the regional SVDs, the SST and rainfall patterns in the first dominant mode (not shown) can be identified feature for feature with the first global SVD in the AA-monsoon domain shown in Figs. 2c and d. Using the same interpretation as before, the basin-scale SST impact (55.8% squared covariance) is very large during austral summer (Table 2), nearly twice that for boreal summer. In contrast to the boreal summer monsoon, there appears to be only one dominant regional coupled mode i.e., the second SVD, which explains 12.3% of the squared covariance. Some of the aforementioned regional features not found in the global SVD, are captured in the 2nd regional SVD (not shown). The remaining SVDs contribute much less (6%) to the covariance. The DJF cumulative rainfall anomaly correlation for individual years (Fig. 4) shows that the influence of the basin-scale SST on the austral monsoon (blue bar) varies over a

wide range between 0.2 to 0.7. The influence of basin-scale SST on the 1997-98 austral summer monsoon rainfall is exceedingly strong as indicated by a very high anomaly correlation ($\approx$ 0.75), which is by far the highest in the 19-year record. The basin-scale SST influence is the second largest ($\approx$0.45) during the 1982-83 El Niño.

5. Summary and conclusion

We have assessed the impacts of basin scale SST, regional coupled processes and internal dynamics on the observed 1997-98 AA-monsoon anomalies using 19 years of rainfall and SST records. Global and regional SVD analyses of SST and rainfall are both carried out. Results reveal a dominant, large-scale monsoon-El Niño coupled mode with well-defined centers of action in the near-equatorial monsoon regions during the boreal summer and winter respectively. Using cumulative anomaly correlation by regional SVDs with observed rainfall, an upper limit of potential predictability for the AA-monsoon region has been defined. On the average, approximately 49% (54%) of the boreal (austral) summer monsoon variability is potentially predictable. The observed 1997-98 AA-monsoon anomalies are found to be very complex with approximately 34% of the anomalies of the Asian (boreal) summer monsoon and 74% of the Australia (austral) monsoon attributable to basin-scale SST influence associated with El Niño. Regional coupled processes contribute an additional 19% and 10%, leaving about 47% and 16% due to internal dynamics for the boreal and austral monsoon respectively. While potential predictability stemming from basin-scale SST influence is generally enhanced during most past El Niños, the highest predictability for the Asian monsoon is found in non-El Niño years (such as 1980 and 1988) when contributions from regional processes far exceed that due to basin-scale SST.

It is important to point out that the statistics shown here are for the monsoon region as a whole and that El Niño impacts seem to be more robust over large span of oceanic regions with well-defined centers of action. As a result, rainfall anomalies averaged over subcontinental regions such as all-India, or arbitrarily chosen land regions over East Asia, which are not near the centers of influence from El Niño, are subject to strong regional effects and large internal variability. These geographic regions while important socio-economically, are *not* necessarily representative of the response of the entire monsoon region to El Niño. Predictability over these subcontinental domains is likely to be even more limited and required additional assessment which are outside the scope of this work.

Finally, we note that 1997 and 1998 witnessed the highest annual global mean temperature record in the past four decades. In a recent study, Lau and Weng (1998) find that the high global mean temperature observed during 1997 might have resulted from a combination of an El Niño effect plus a warming tendency attributable to a strong decadal-to-interdecadal oscillation and a global warming trend since the 1950's. They observe that the long-term warming has a strong signature in the Indian Ocean. These global changes could have modified the tropical climate state and altered the way the three fundamental factors (basin-scale SST, regional coupled processes and internal dynamics) interact thus affecting the potential predictability of the total monsoon system. Results of this paper suggest that enhanced monsoon predictability requires better understanding of not only monsoon-El Niño relationship, but also regional coupled processes and their modulation by long-term climate change.

11

Acknowledgement

Table 1 Percentage of squared covariance explained by the first five global and regional SVDs of monthly rainfall and SST for MJJAS

	SVD1	SVD2	SVD3	SVD4	SVD5
Global	58.4	7.9	7.1	3.3	2.4
Regional	29.3	15.8	12.7	7.2	5.1

Table 2. Percentage of squared variance explained by the first five global and regional SVDs of monthly rainfall and SST for ONDJF

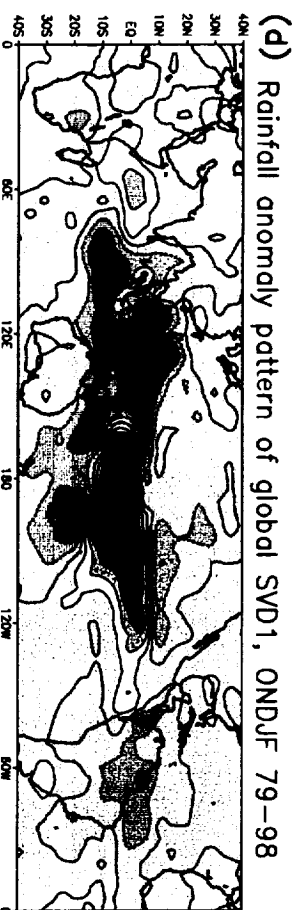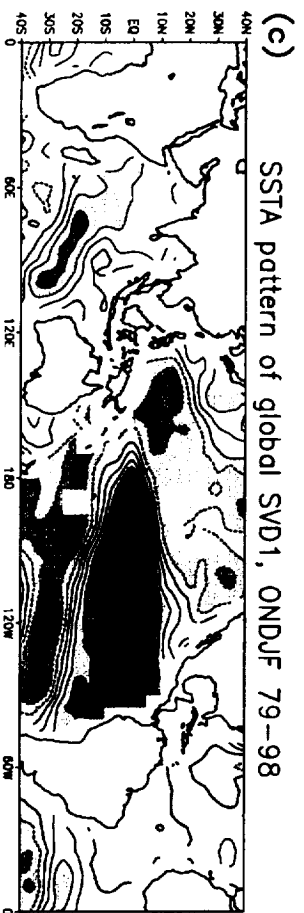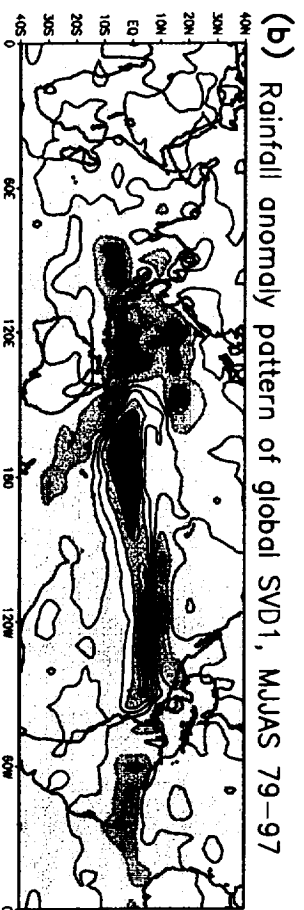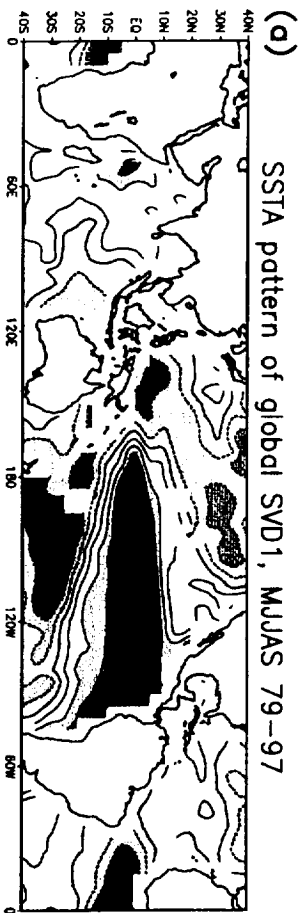|	SVD1	SVD2	SVD3	SVD4	SVD5
Global	74.6	6.6	2.9	1.7	1.5
Regional	55.8	12.3	6.3	4.2	3.5

FIGURE CAPTIONS

Figure 1 Observed anomalies in (a) SST and (b) rainfall for JJA, 1997 and (c) SST and (b) rainfall for DJF, 1997-98. Units of rainfall are in mm/day and SST in °C .

Figure 2 Spatial pattern of the first global SVD for (a) SST and (b) rainfall anomalies for MJJAS, and (c) SST and (d) rainfall anomalies for ONDJF. Units of rainfall are in mm/day and SST in °C .

Figure 3 Bar chart showing cumulative anomaly correlation of the first five regional SVD modes with the observed JJA rainfall over entire Asia-Australia domain. Bars are color-coded with first to fifth SVDs in blue, orange, green, red and yellow respectively.

Figure 4 Same as in Fig. 3, except for DJF.

(a) SSTA   JJA 1997

(b) GPCP Precipitation anomaly JJA 1997

(c) SSTA   DJF 1997-98

(d) GPCP Precipitation anomaly DJF 1997-98

(a) SSTA pattern of global SVD1, MJJAS 79–97

(b) Rainfall anomaly pattern of global SVD1, MJJAS 79–97

(c) SSTA pattern of global SVD1, ONDJF 79–98

(d) Rainfall anomaly pattern of global SVD1, ONDJF 79–98
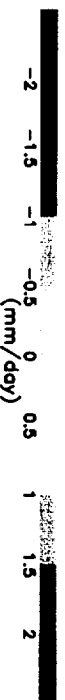
Correlation of reconstructed rainall anomaly (1 to 5 SVDs) with observation for JJA for AAM region
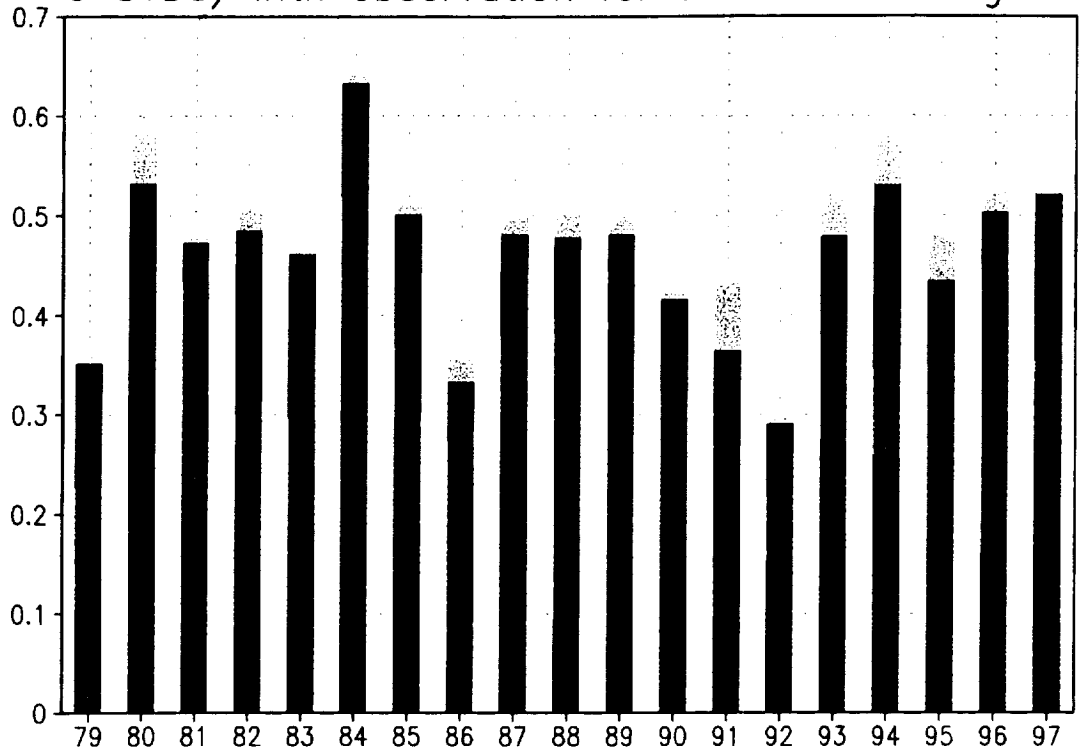
Correlation of reconstructed rainall anomaly (1 to 5 SVDs) with observation for DJF for AAM region